

# Analysis of optical nonlinearity by defect states in one-dimensional photonic crystals

Toshiaki Hattori, Noriaki Tsurumachi, and Hiroki Nakatsuka

*Institute of Applied Physics, University of Tsukuba, Tsukuba 305, Japan*

Received January 31, 1996; revised manuscript received June 10, 1996

Enhancement of optical nonlinearity in one-dimensional photonic-crystal structures with a defect is considered theoretically. It is shown that a large enhancement can be obtained for absorption saturation and degenerate four-wave mixing efficiency as a result of large optical field amplitude of the localized photonic-defect mode at the defect layer. The figure of merit of the use of the photonic-crystal structure is derived especially for systems in which the concentration of the nonlinear optical material can be arbitrarily adjusted. Optical bistability is also predicted for optically dense samples. They can be applied in real photonic devices because of their simple structure and the large enhancement obtained. © 1997 Optical Society of America [S0740-3224(97)00802-3]

## 1. INTRODUCTION

Control of photon modes by photonic-crystal (PC) structures is expected to be a key technology for future photonic devices. Much attention has been paid to the control of spontaneous emission in PC structures.<sup>1</sup> One of its important goals is a thresholdless laser, which would be available by placing a light-emitting center in a defect in a three-dimensional PC structure, which has three-dimensionally periodical dielectric-constant modulation. For this type of devices, however, fabrication of the three-dimensional structure with a period on the scale of visible or near-infrared wavelengths is still a hard task. Nonlinear optical devices that use a PC structure are also interesting targets. Low-threshold optical switching<sup>2</sup> and nonlinear optical diodes<sup>3</sup> that use optical nonlinearity of one-dimensional (1-D) PC structures have been proposed. In these proposals the optical nonlinearity of the systems is assumed to be distributed through the PC structure.

Large enhancement of optical nonlinearity, however, can be achieved more easily by use of the high local field of a localized photonic state at a defect in a 1-D PC structure. Since local light intensity can be made very high at the defect by making use of the localized photonic-defect mode, the optical nonlinearity of the material at the defect can be effectively enhanced by many orders of magnitude.<sup>4</sup> For this purpose the 1-D structure is the best candidate since the incident field is fully coupled to the local mode only in 1-D structures. Devices that use this scheme can be fabricated easily simply by placing thin-film nonlinear optical material in a 1-D PC structure, and we have obtained preliminary results on the enhancement of optical nonlinearity in a system of a dye-doped polymer film in a multilayer dielectric structure.<sup>5</sup> This technique is promising especially for applications such as dynamic holography, optical phase conjugation, and two-dimensional optical signal processing, when thin-film nonlinear optical material is used.

In this paper we will treat a multilayer stack of dielectrics with a defect layer at the center as a model structure and describe the advantage of the use of this structure in

comparison with a simple monolayer nonlinear optical film. Input-intensity dependence of the transmittance and the efficiency of the degenerate four-wave mixing will be analyzed, and fundamental expressions which are useful for experimental comparison will be derived. Optical bistability, as a special case of the input-intensity dependence of the transmittance, will also be described.

## 2. INTENSITY-DEPENDENT TRANSMITTANCE

Quarter-wave stacks of two dielectrics with different refractive indices, which have long been used for mirrors or optical filters, are good examples of 1-D PC's. They can have a wide photonic band gap at the frequency where Bragg reflection takes place. By placing a structural defect at the center of the stack, a photonic-defect state that is localized around the defect can be made. Intensity dependence of the transmittance of such PC structures with a defect is theoretically considered based on the model structure shown in Fig. 1. The central layer, X, is the defect layer, which has finite absorption. On both sides of the defect layer are  $N$  bilayers of A and B, which are on substrates S. The refractive indices of these layers are assumed to be  $n_A = 1.46$  and  $n_B = 2.35$ , which are the values for silica and titania, respectively. This structure can be easily made by vacuum deposition. The refractive index of the defect layer,  $n_X$ , is assumed to be 1.5. The substrates are made of glass, and the refractive index of them is assumed, for the convenience of the calculation, to be equal to that of the defect layer. The layer thicknesses of the periodical part and the defect layer,  $d_A$ ,  $d_B$ , and  $d_X$ , are assumed to satisfy  $n_A d_A = n_B d_B = n_X d_X / 2$ . In this case the transmission peak induced by a photonic-defect state appears at the center of the band gap (midgap position).

Calculated transmission spectrum for  $N = 5$ ,  $\kappa = 0.003$ , and  $n_A d_A = 640 \text{ nm}/4$  is shown in Fig. 2, where  $\kappa$  is the extinction coefficient of the defect layer. The width (FWHM) of the transmission peak is 3.6 nm. When  $\kappa = 0$ , the transmittance at the midgap frequency

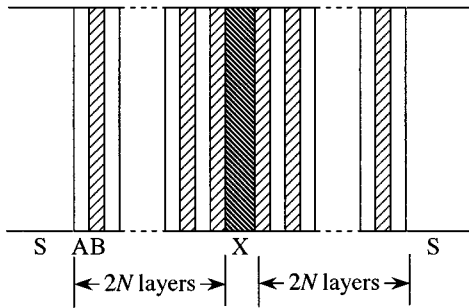
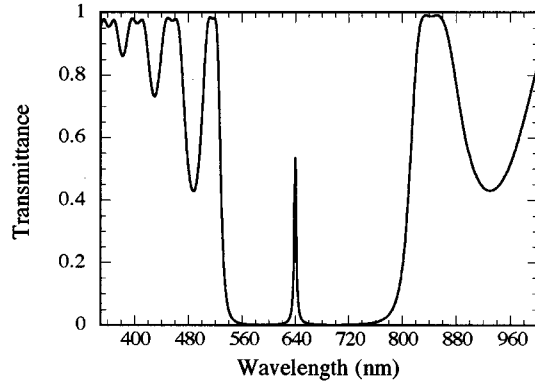


Fig. 1. Model of 1-D PC structures.

Fig. 2. Calculated transmission spectrum of a 1-D PC with a defect with  $N = 5$ ,  $\kappa = 0.003$ , and  $n_A d_A = 640 \text{ nm}/4$ .

is unity. In the figure it is decreased to  $\sim 50\%$  because of the finite absorption. The value of  $N = 5$  is a feasible one, and most of the calculation in the discussion below will be based on this value. When the optical thickness of the defect layer,  $n_X d_X$ , is slightly changed from twice that of the periodical part, the position of the peak is shifted accordingly. In experiments the peak wavelength can be tuned by use of this fact.<sup>5</sup> The transmission spectrum and the local light intensity can be calculated by the method of characteristic matrices.<sup>6</sup>

A calculated field pattern of light at the frequency of the midgap transmission peak that is incident normally upon this PC structure with  $N = 5$  and no absorbance of the defect layer is shown in Fig. 3. The input light amplitude is normalized to unity in this figure. It can be seen that the local field amplitude at the central defect layer is greatly enhanced compared with the incident field amplitude. The peak amplitude is calculated to be  $(n_B/n_A)^N$ , which is equal to 10.8 for  $N = 5$ . From this fact, large optical nonlinearity is expected when an optically nonlinear medium is placed at the central defect layer.

The transmission coefficient of the light field,  $t$ , at the midgap frequency with finite absorption of the defect layer is calculated as

$$t = \frac{-2}{2 \cosh\left(\frac{\pi\kappa}{n_X}\right) + \sinh\left(\frac{\pi\kappa}{n_X}\right) \left[ \frac{(n_B/n_A)^{2N}}{1 + i\kappa/n_X} + \frac{1 + i\kappa/n_X}{(n_B/n_A)^{2N}} \right]}, \quad (1)$$

and the transmittance,  $T$ , is

$$T = |t|^2. \quad (2)$$

The spatially averaged intensity of light in the defect layer, supposing the input intensity is unity, is calculated as

$$G = T \frac{n_X}{2\pi\kappa} \sinh\left(\frac{\pi\kappa}{n_X}\right) \left\{ \cosh\left(\frac{\pi\kappa}{n_X}\right) \left[ \left(\frac{n_B}{n_A}\right)^{2N} \frac{n_X^2}{n_X^2 + \kappa^2} + \left(\frac{n_A}{n_B}\right)^{2N} \right] + \sinh\left(\frac{\pi\kappa}{n_X}\right) \frac{2n_X^2}{n_X^2 + \kappa^2} \right\}. \quad (3)$$

For large  $N$  such that

$$(n_B/n_A)^N \gg 1, \quad (4)$$

these expressions can be simplified as

$$t = \frac{-2}{2 + \frac{\pi\kappa}{n_X} \left(\frac{n_B}{n_A}\right)^{2N}}, \quad (5)$$

$$T = \frac{4}{\left[2 + \frac{\pi\kappa}{n_X} \left(\frac{n_B}{n_A}\right)^{2N}\right]^2}, \quad (6)$$

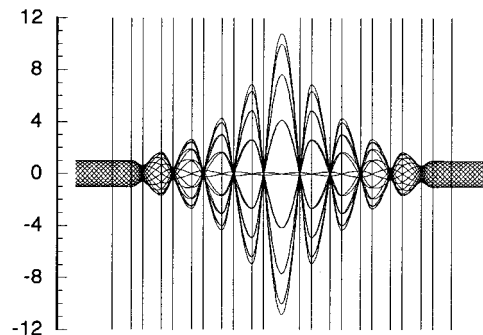
$$G = \frac{T}{2} \left(\frac{n_B}{n_A}\right)^{2N}, \quad (7)$$

where it is assumed that

$$n_X \gg \kappa. \quad (8)$$

Calculation with the exact expressions, Eqs. (1)–(3), shows that the approximate forms, Eqs. (5)–(7), yield results good enough for the following discussion when  $N \geq 3$ .

The optical nonlinearity is assumed to be purely absorptive and to originate from absorption saturation in the defect layer. The absorption centers can be general at this point, although detailed discussion on the optimization of the nonlinearity will be given later on systems in which the concentration of the absorption centers can be arbitrarily controlled. The pure absorptive nonlinearity can be justified supposing that the midgap frequency falls in the central region of the absorption band and that the dispersive contribution is small. This point is in contrast to some reported cases of nonlinear Fabry–Perot étalons, where the major contribution to the nonlinear transmit-

Fig. 3. Calculated field pattern of light at the frequency of the midgap transmission peak that is incident normally upon the PC structure with  $N = 5$  and with no absorbance of the defect layer.

tance change is thought to be by dispersive nonlinearity.<sup>7-9</sup> The absorption of the defect layer is assumed to be saturated as

$$\kappa = \frac{\kappa_0}{1 + I/I_S}. \quad (9)$$

Here,  $I$  is the local intensity of light and  $I_S$  is the saturation intensity.

When a mean field approximation is adopted, i.e., the local intensity that appears in Eq. (9) is assumed to be independent of the position in the defect layer as

$$I = GI_{\text{in}}, \quad (10)$$

where  $I_{\text{in}}$  is the input intensity, then Eqs. (6), (7), (9), and (10) are combined and lead to

$$(y_0 - y)(y + 2)^2 - xy = 0, \quad (11)$$

with

$$x \equiv 2 \left( \frac{n_B}{n_A} \right)^{2N} \frac{I_{\text{in}}}{I_S}, \quad (12)$$

$$y \equiv \frac{\pi}{n_X} \left( \frac{n_B}{n_A} \right)^{2N} \kappa, \quad (13)$$

$$y_0 \equiv \frac{\pi}{n_X} \left( \frac{n_B}{n_A} \right)^{2N} \kappa_0, \quad (14)$$

$$T = \frac{4}{(y + 2)^2}. \quad (15)$$

Equation (11) exhibits bistability for  $y_0 > 16$  or for unsaturated transmittance less than 1/81. This result is essentially the same as that obtained by Szöke *et al.* for nonlinear Fabry–Perot cavities.<sup>10</sup> The mean field approximation, however, is not good for solid samples. As can be seen from Fig. 3, the light intensity is highest at the center of the defect layer, and almost zero at the boundaries. Thus the absorption is saturated most strongly at the center, and the absorption change of the central position affects the transmittance most effectively. This spatial hole-burning effect should be taken into account for correct treatment.

If the peak transmittance of a PC structure with larger  $N$  is assumed to be not much smaller than unity, the magnitude of  $\kappa$  is of the order of  $(n_A/n_B)^{2N}$ , as seen from Eq. (6). The absorbed fraction of light for each round trip of the cavity made by the defect is of the same order as  $\kappa$ . In this case the saturated extinction coefficient, which is dependent on the position, can be safely replaced by a position-independent effective value in calculation of quantities such as the transmittance and the spatial profile of the light intensity, and the spatial profile of light in the defect layer without absorption can be used for that with absorption.

The spatial intensity profile of light in the defect layer can be approximated as

$$I(z) = 2GI_{\text{in}} \cos^2(\pi z/d_X)(-d_X/2 < z < d_X/2). \quad (16)$$

Here,  $z$  is the position in the defect layer along the direction normal to the layer surface. The saturated extinction coefficient is dependent on the position as

$$\kappa(z) = \frac{\kappa_0}{1 + I(z)/I_S}, \quad (17)$$

where  $I_S$  is the saturation intensity of the raw material. Since the effect of the absorption change to the transmittance is also proportional to the local intensity, the effective extinction coefficient is expressed as

$$\bar{\kappa} = \frac{\int_{-d_X/2}^{d_X/2} \kappa(z)I(z)dz}{\int_{-d_X/2}^{d_X/2} I(z)dz} = \kappa_0 \frac{2(\sqrt{1+p} - 1)}{p\sqrt{1+p}}, \quad (18)$$

with

$$p \equiv 2GI_{\text{in}}/I_S. \quad (19)$$

We will use the functional form of Eq. (18) only in the discussion of optical bistability below, and for discussions on the enhancement of the optical nonlinearity of PC structures we will use only the lowest-order response:

$$\frac{d\bar{\kappa}}{dI_{\text{in}}} = -\frac{3}{2} \kappa G/I_S. \quad (20)$$

Here  $\kappa$  and  $G$  are the values for small input light. In the discussion of the small-input response below,  $\kappa$  will be used instead of  $\kappa_0$ , where the distinction between them is of no significance. The expression above shows that absorption saturation, when the spatial hole-burning effect is taken into account, is 3/2 times as effective as the result of the mean-field approximation, as seen from Eqs. (9) and (10). When the transmittance is appreciably changed by absorption saturation, the dependence of the transmittance on the input intensity is not linear. However, it can be regarded as almost linear up to the effective saturation intensity, where the saturation is half that for infinite input intensity. Thus the effective saturation intensity can be analyzed by calculating the lowest-order dependence.

Transmittance change for weak input is calculated as

$$\frac{dT}{dI_{\text{in}}} = \frac{dT}{d\bar{\kappa}} \frac{d\bar{\kappa}}{dI_{\text{in}}} = \frac{1}{I_S} \frac{24\pi\kappa}{n_X} \left( \frac{n_B}{n_A} \right)^{4N} \left[ 2 + \frac{\pi\kappa}{n_X} \left( \frac{n_B}{n_A} \right)^{2N} \right]^{-5}. \quad (21)$$

For the convenience of further discussion the notation below is introduced:

$$\Delta \equiv \frac{dT}{dI_{\text{in}}} I_S. \quad (22)$$

This quantity is a measure of the magnitude of the nonlinearity of transmittance of the sample normalized by the nonlinearity of the raw material. With this notation, for the PC structure,

$$\Delta_{\text{PC}} = \frac{24\pi\kappa}{n_X} \left( \frac{n_B}{n_A} \right)^{4N} \left[ 2 + \frac{\pi\kappa}{n_X} \left( \frac{n_B}{n_A} \right)^{2N} \right]^{-5}. \quad (23)$$

This is plotted  $N = 5$  in Fig. 4. It can be seen that the maximum transmittance change is obtained by a relatively small value of  $\kappa$  and that  $\kappa$  larger than several times the optimal value gives a significantly small nonlinear optical effect.

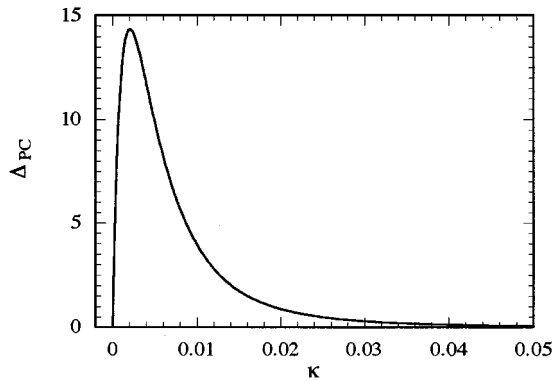


Fig. 4. Normalized transmittance change of the PC sample with  $N = 5$  plotted as a function of the extinction coefficient as obtained in Eq. (23).

To compare the optical nonlinearity of a PC sample, using these expressions, with that of a naked sample, i.e., a simple monolayer film of the nonlinear material, we calculate the transmittance change of a simple film due to absorption saturation. When boundary reflection can be neglected, the weak-signal nonlinear transmittance change of a film with extinction coefficient  $\kappa'$  and saturation intensity  $I_S$  is calculated as

$$\Delta_{\text{naked}} = \exp(-\alpha'L)[1 - \exp(-\alpha'L)]. \quad (24)$$

Here,  $L$  is the thickness of the film, and the absorption coefficient  $\alpha'$  is related to the extinction coefficient as

$$\alpha' = \frac{4\pi\kappa'}{\lambda}, \quad (25)$$

where  $\lambda$  is the wavelength of the light in vacuum.

For samples with very small absorption such that

$$\kappa \ll (n_X/\pi)(n_A/n_B)^{2N} \quad (26)$$

or

$$\alpha'L \ll 1, \quad (27)$$

the transmittance change is

$$\Delta_{\text{PC}} = \frac{3\pi\kappa}{4n_X} \left(\frac{n_B}{n_A}\right)^{4N} \quad (28)$$

for PC samples and

$$\Delta_{\text{naked}} = \frac{4\pi\kappa'L}{\lambda} \quad (29)$$

for naked films. Since the thickness of the central defect layer is  $L = \lambda/2n_X$ , the enhancement factor of the effective nonlinear susceptibility of a half-wavelength film in the PC structure compared with the same film without the PC structure is

$$\mathcal{F} \equiv \Delta_{\text{PC}}/\Delta_{\text{naked}} = \frac{3}{8} \left(\frac{n_B}{n_A}\right)^{4N}. \quad (30)$$

This factor is proportional to the fourth power of the field-enhancement factor,  $(n_B/n_A)^N$ . This can be explained as follows. The excited-state population, which causes the absorption saturation, is proportional to the local intensity, or to  $(n_B/n_A)^{2N}$ . The third-order polarization is proportional to the product of the excited-state

population and the local-field amplitude, i.e., to  $(n_B/n_A)^{3N}$ . Emission intensity due to the third-order polarization is proportional to the product of the third-order polarization and the local-field amplitude, i.e., to  $(n_B/n_A)^{4N}$ . In short, the transmitted intensity change is proportional to the fourth power of the local-field amplitude irrespective of whether the nonlinear medium is in a PC structure or not. From the expression above, nonlinearity enhancement as high as 5100 is expected for a PC sample with  $N = 5$ . For materials with fixed nonlinearity this is the figure of merit expected by the use of the PC structure.

For samples such as dye-doped polymer films, however, the concentration of the nonlinear material can be optimized for the maximum optical nonlinear effect. A naked sample with a small extinction coefficient that satisfies Eq. (26) with  $N = 5$  has transmittance greater than 98%. It is not realistic to compare nonlinearity of samples with such a low concentration. To understand the advantage of using the PC structure as nonlinear optical elements, one has to compare the nonlinearity of samples with the optimized concentration of the nonlinear material in each structure. For samples with finite absorption, the intensity enhancement factor,  $G$ , is greatly suppressed by the absorption in the nonlinear layer, and the (linear) transmittance is also suppressed by the absorption, as given in Eqs. (6) and (7). Dependence of the value  $G$  on the extinction coefficient  $\kappa$  is plotted in Fig. 5 for the PC structure of  $N = 5$ . It can be seen that the intensity enhancement rapidly decreases when  $\kappa$  is increased and that  $\kappa$  should be kept low enough to fully make use of the light-field enhancement at the defect layer. Since the nonlinear susceptibility for absorption saturation is proportional to the density of the dye, i.e., proportional to the absorption coefficient, the largest nonlinearity in transmittance for fixed number of layers is realized by optimizing the absorption coefficient.

Maximization of either the transmittance change,  $\Delta$ , or the ratio of the change in the transmitted intensity to the linearly transmitted intensity,  $\Delta/T$ , can be more relevant for the supposed purpose. Maximization of  $\Delta$  is achieved by setting

$$\kappa = \frac{n_X}{2\pi} \left(\frac{n_A}{n_B}\right)^{2N}, \quad (31)$$

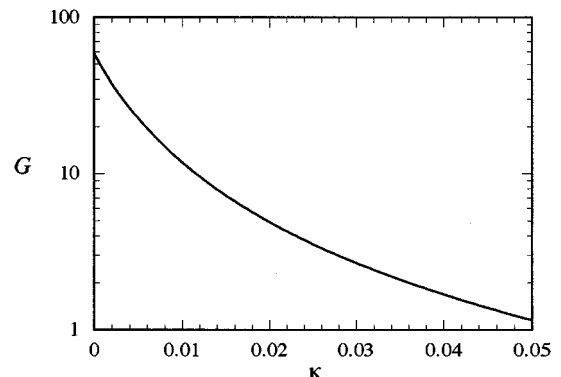


Fig. 5. Dependence of the intensity-enhancement factor  $G$  on the extinction coefficient  $\kappa$  for the PC structure of  $N = 5$ .

or

$$T = 0.64, \tag{32}$$

and the maximized value is

$$\Delta_{PC}^{\max} = \frac{384}{3125} \left(\frac{n_B}{n_A}\right)^{2N}. \tag{33}$$

For naked films, on the other hand, maximum value of

$$\Delta_{\text{naked}}^{\max} = \frac{1}{4} \tag{34}$$

is obtained for  $\alpha'L = \ln 2$ . By comparing these optimized values, the enhancement of the nonlinear susceptibility is

$$\mathcal{F}_\Delta \equiv \Delta_{PC}^{\max}/\Delta_{\text{naked}}^{\max} = \frac{1536}{3125} \left(\frac{n_B}{n_A}\right)^{2N}. \tag{35}$$

In a similar way,  $\Delta/T$  is maximized for the PC structure by setting

$$\kappa = \frac{n_X}{\pi} \left(\frac{n_A}{n_B}\right)^{2N}, \tag{36}$$

or

$$T = 4/9, \tag{37}$$

and the maximized value is

$$\left(\frac{\Delta}{T}\right)_{PC}^{\max} = \frac{2}{9} \left(\frac{n_B}{n_A}\right)^{2N}. \tag{38}$$

For naked films the maximum value of

$$\left(\frac{\Delta}{T}\right)_{\text{naked}}^{\max} = 1 \tag{39}$$

is obtained for  $\alpha'L = \infty$ , or  $T = 0$ . Even for a more realistic value of the transmittance of, e.g., 10%, as much as 90% of the value shown in Eq. (39) is obtained. The enhancement of the nonlinear susceptibility is

$$\mathcal{F}_{\Delta/T} \equiv \left(\frac{\Delta}{T}\right)_{PC}^{\max} / \left(\frac{\Delta}{T}\right)_{\text{naked}}^{\max} = \frac{2}{9} \left(\frac{n_B}{n_A}\right)^{2N}. \tag{40}$$

In either case of Eq. (35) or Eq. (40) the enhancement of the nonlinear transmission change by use of the PC structure is proportional to  $(n_B/n_A)^{2N}$ , and enhancement factors of 57 and 26, for  $\Delta$  and  $\Delta/T$ , respectively, are expected for an  $N = 5$  structure or 6700 and 3000 for  $N = 10$ .

The dependence of  $(n_B/n_A)^{2N}$  can be understood as follows. The local light intensity enhancement at the defect layer is proportional to  $(n_B/n_A)^{2N}$ , which can be regarded as an effective  $Q$  value of the microcavity made by the defect. The nonlinearity of the raw material, however, should be kept of the order of  $(n_A/n_B)^{2N}$  to fully make use of the enhancement. The consequent amount of the change in the extinction coefficient is of the order of unity. The effect of this change on the transmitted intensity, however, is again proportional to the intensity enhancement,  $(n_B/n_A)^{2N}$ . Thus the finally obtained enhancement factor of the effective nonlinearity is proportional to  $(n_B/n_A)^{2N}$ . From another point of view, for samples with similar transmittance, the nonlinearity enhancement is

only due to the reduction of the effective saturation intensity, which is inversely proportional to the local intensity enhancement at the defect layer.

The comparison between the optimized nonlinearity described above shows the potential of the use of PC structure in nonlinear optical elements. For experimental demonstration, however, it is more straightforward to compare the magnitude of the nonlinearity of PC and naked samples with the same transmittance. If the inside structure of the nonlinear optical elements is not known, transmittance is the only quantity characterizing the (linear) property of the elements. Equations (23) and (24) are rewritten as a function of the transmittance as

$$\Delta_{PC}(T) = \frac{3}{2} \left(\frac{n_B}{n_A}\right)^{2N} T^2(1 - \sqrt{T}), \tag{41}$$

$$\Delta_{\text{naked}}(T) = T(1 - T). \tag{42}$$

These are plotted for  $N = 5$  in Fig. 6. The nonlinearity enhancement factor is

$$\mathcal{F}(T) \equiv \Delta_{PC}(T)/\Delta_{\text{naked}}(T) = \frac{3}{2} \left(\frac{n_B}{n_A}\right)^{2N} \frac{T}{1 + \sqrt{T}}, \tag{43}$$

which is plotted for  $N = 5$  in Fig. 7. It is seen from the figure that the enhancement is larger as the transmit-

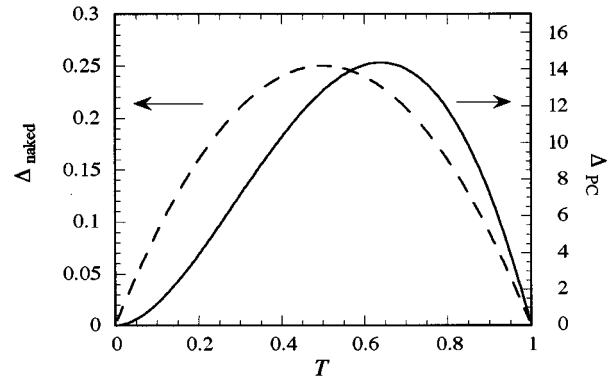


Fig. 6. Normalized transmittance change for the PC sample with  $N = 5$  and for a naked sample plotted as a function of the linear transmittance.

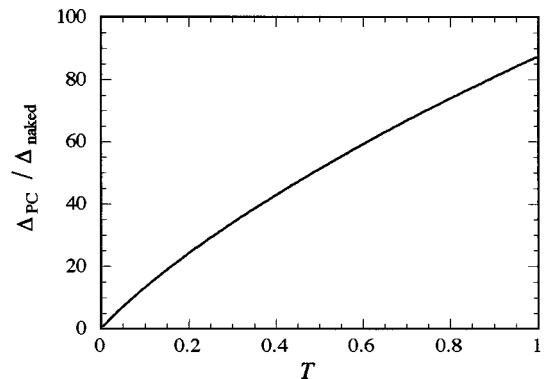


Fig. 7. Ratio of the normalized transmittance change for the PC sample with  $N = 5$  and that for a naked sample, plotted as a function of the linear transmittance.

tance is larger, although the nonlinearity as shown in Fig. 6 becomes small for large transmittance. Reasonable enhancement, as high as about half of the maximum, can be obtained for transmittance of  $\sim 50\%$ , where the absolute value of the nonlinearity takes values close to the maximum. Thus the obtained enhancement factor is proportional to  $(n_B/n_A)^{2N}$  and  $\sim 50$  for  $N = 5$  samples.

The determination of the number of the PC structure bilayers,  $N$ , is important for practical applications. Since the peak width is proportional to  $(n_A/n_B)^{2N}$ , fluctuation in the layer thickness, or the spectral width of the light utilized, can limit the practical number of layers, which determines the achievable enhancement in optical nonlinearity. The value of  $N = 5$ , as used in the preceding discussions, is very feasible, as seen from Fig. 2, and even the value of  $N = 10$  is not difficult when a narrow-band laser is used.

In the preceding description, the weak-field response is mainly discussed. When the input intensity is high, however, it can be shown that optical bistability can be observed. Combining Eqs. (6), (7), (18), and (19), we obtain following expressions, which are similar to Eqs. (11)–(15);

$$\left[ y_0 - \frac{1}{4} (y + \sqrt{y^2 + 8y_0y}) \right] (y + 2)^2 - xy = 0, \quad (44)$$

with

$$x \equiv 2 \left( \frac{n_B}{n_A} \right)^{2N} \frac{I_{\text{in}}}{I_S}, \quad (45)$$

$$y \equiv \frac{\pi}{n_X} \left( \frac{n_B}{n_A} \right)^{2N} \bar{\kappa}, \quad (46)$$

$$y_0 \equiv \frac{\pi}{n_X} \left( \frac{n_B}{n_A} \right)^{2N} \kappa_0, \quad (47)$$

$$T = \frac{4}{(y + 2)^2}. \quad (48)$$

The relation between the input intensity and the transmittance is plotted in Fig. 8 for several values of  $y_0$ , which characterizes the linear transmittance by Eq. (48). Optical bistability is observed for  $y_0 > 20$ . The range of the normalized input intensity,  $x$ , where bistability is observed, is numerically calculated as a function of the linear transmittance,  $T_0$ , which is shown in Fig. 9. The general trend of the relation between the input intensity and the transmittance is very similar to that obtained from Eqs. (11)–(15), which results from the mean-field theory. Multistability is not observed, and the bistability appears only in a single region of input intensity for large enough values of  $y_0$ , which is in contrast with systems in which dispersive nonlinearity is more effective than absorptive nonlinearity.

### 3. FOUR-WAVE MIXING EFFICIENCY

Efficiency of various nonlinear optical processes other than the intensity-dependent transmittance discussed above can be enhanced by the PC structure. In this sec-

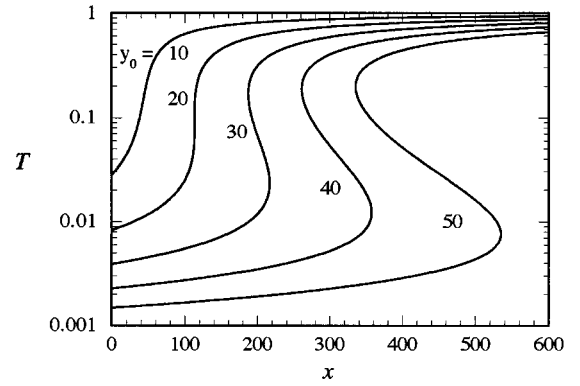


Fig. 8. Relation between the input intensity and the transmittance for several values of  $y_0$ , which characterizes the magnitude of the linear transmittance.

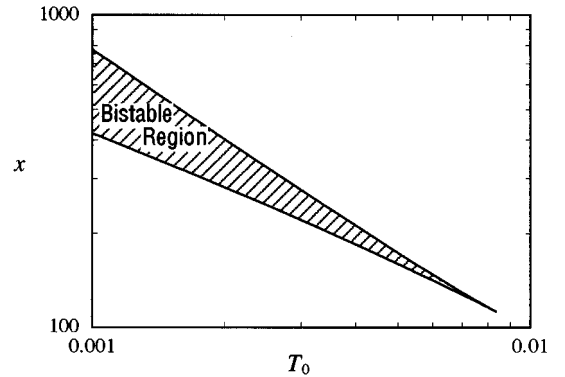


Fig. 9. Range of the normalized input intensity,  $x$ , where bistability is observed, as a function of the linear transmittance,  $T_0$ .

tion the efficiency of degenerate four-wave mixing (DFWM) is considered, in which three beams with wave vectors of  $\mathbf{k}_1$ ,  $\mathbf{k}_2$ , and  $\mathbf{k}_3$  are incident upon the sample and the intensity of the diffracted beam in the direction of  $\mathbf{k}_1 + \mathbf{k}_2 - \mathbf{k}_3$  is measured. Signal processing with DFWM is one of the major possible application of thin-film nonlinear materials as used in this study. Phase-conjugated wave generation and dynamic holography can also be regarded as DFWM processes.

The intensity-dependent transmittance change is, to the lowest order, also a third-order nonlinear optical process, as is DFWM, and can be treated in the same framework. The transmitted light field can be expressed as a sum of the linearly transmitted field and the field generated by the third-order polarization as

$$\mathbf{E}_{\text{out}} = \mathbf{E}_{\text{out}}^{(1)} + \mathbf{E}_{\text{out}}^{(3)}. \quad (49)$$

For the observation of the intensity-dependent transmittance a single beam is used as the input. Consequently, all of the output field has the same wave vector as that of the input. The third-order field contributes to the transmittance change by interference with the linear field. In the DFWM process, on the other hand, the two or three input beams have different wave vectors, and the wave vector of the third-order field is different from that of any of the input beams. Thus the intensity of the DFWM light is proportional to the squared magnitude of the third-order output field. Since under the condition of Eq.

(8) the transmission coefficient is always real and the sign of it does not change, the output intensity in the single-beam configuration is expressed as

$$I_{\text{out}} = c \epsilon |E_{\text{out}}|^2 = c \epsilon \{ |E_{\text{out}}^{(1)}|^2 + 2 |E_{\text{out}}^{(1)} E_{\text{out}}^{(3)}| \} \quad (50)$$

in the approximation of third-order nonlinearity. The transmittance is

$$T = \frac{I_{\text{out}}}{I_{\text{in}}} = T_0 + 2 \sqrt{T_0} \left| \frac{E_{\text{out}}^{(3)}}{E_{\text{in}}} \right|, \quad (51)$$

where  $E_{\text{in}}$  is the input light field amplitude and  $T_0$  is the linear transmittance, which is used only when distinction from the intensity-dependent transmittance is required. For the derivation of this equation the following relation is used:

$$E_{\text{out}}^{(1)} = \sqrt{T_0} E_{\text{in}}. \quad (52)$$

By differentiating Eq. (51) by  $I_{\text{in}}$ , we obtain

$$\frac{dT}{dI_{\text{in}}} = 2 \sqrt{T_0} \frac{d}{dI_{\text{in}}} \left| \frac{E_{\text{out}}^{(3)}}{E_{\text{in}}} \right|. \quad (53)$$

Since  $E_{\text{out}}^{(3)}/E_{\text{in}}$  should be proportional to  $I_{\text{in}}$ ,

$$|E_{\text{out}}^{(3)}| = \frac{I_{\text{in}}}{2 \sqrt{T_0}} \frac{dT}{dI_{\text{in}}} |E_{\text{in}}|. \quad (54)$$

The DFWM intensity can be obtained from this relation as

$$I_{\text{DFWM}} = \frac{1}{4T} \left( \frac{dT}{dI_{\text{in}}} \right)^2 I_{\text{in}}^3. \quad (55)$$

This equation generally relates the magnitude of the nonlinear transmission to the DFWM intensity.

When notation

$$\mathcal{W} \equiv I_{\text{DFWM}} I_S^2 / I_{\text{in}}^3 \quad (56)$$

is introduced for the normalized DFWM generation efficiency, it is expressed as a function of the linear transmittance as

$$\mathcal{W}_{\text{PC}} = \frac{9}{16} \left( \frac{n_B}{n_A} \right)^{4N} T^3 (1 - \sqrt{T})^2 \quad (57)$$

for PC structures and

$$\mathcal{W}_{\text{naked}} = \frac{1}{4} T (1 - T)^2 \quad (58)$$

for naked samples. They are shown for  $N = 5$  in Fig. 10. They have maximum values when  $T = 9/16$  and  $T = 1/3$  for PC and naked samples, respectively. The ratio is also plotted as a function of the linear transmittance in Fig. 11. The general behavior is similar to the  $T$  dependence of  $\Delta$ , as shown in Figs. 6 and 7. The enhancement in the DFWM intensity is larger as the transmittance is larger, although the nonlinearity as shown in Fig. 10 becomes small for large transmittance. Reasonable enhancement, as high as about one third of the maximum, can be obtained for transmittance of  $\sim 50\%$ , where the absolute value of the nonlinearity takes values close to the

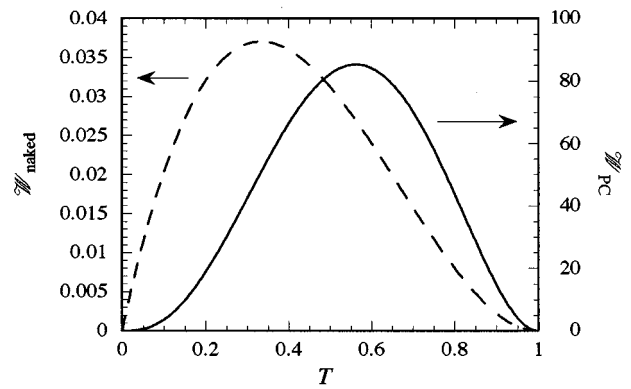


Fig. 10. Normalized DFWM generation efficiency for the PC sample with  $N = 5$  and for a naked sample plotted as a function of the linear transmittance.

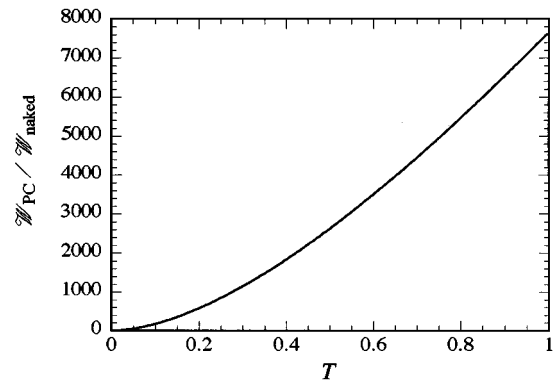


Fig. 11. Ratio of the normalized DFWM generation efficiency for the PC sample with  $N = 5$  and that for a naked sample, plotted as a function of the linear transmittance.

maximum. The obtained enhancement factor is proportional to  $(n_B/n_A)^{4N}$  and more than 2000 for  $N = 5$  samples.

#### 4. SUMMARY

In summary, enhancement of optical nonlinearity in 1-D PC structures with a defect was considered theoretically. It is shown that large enhancement can be obtained for absorption saturation and DFWM efficiency as a result of high optical field amplitude of the localized photonic-defect mode at the defect layer. The figure of merit of the use of the PC structure is derived especially for systems in which the concentration of the nonlinear optical material can be arbitrarily adjusted. Optical bistability is also predicted for optically dense samples. They can be applied in real photonic devices because of their simple structure and the large enhancement obtained. We have already obtained preliminary results that are consistent with the theoretical analysis described here.<sup>5</sup>

#### REFERENCES

1. C. M. Soukoulis, ed., *Photonic Band Gaps and Localization* (Plenum, New York, 1993).
2. S. Radic, N. George, and G. P. Agrawal, "Theory of low-threshold optical switching in nonlinear phase-shifted periodic structures," *J. Opt. Soc. Am. B* **12**, 671–680 (1995).

3. M. D. Tocci, M. J. Bloemer, M. Scalora, J. P. Dowling, and C. M. Bowden "Thin-film nonlinear optical diode," *Appl. Phys. Lett.* **66**, 2324–2326 (1995).
4. R. Shimano, S. Inouye, M. Kuwata-Gonokami, T. Nakamura, M. Yamanishi, and I. Ogura "Efficient phase conjugation wave generation from a GaAs single quantum well in a microcavity," *Jpn. J. Appl. Phys.* **34**, L817–L820 (1995).
5. T. Hattori, N. Tsurumachi, N. Muroi, H. Nakatsuka, and E. Ogino, "Enhancement of optical nonlinearity in one-dimensional photonic crystals," *Prog. Crystal Growth Character.* **33**, 183–186 (1996).
6. For example, M. Born and E. Wolf, *Principles of Optics*, 6th ed. (Pergamon, Oxford, 1980).
7. H. M. Gibbs, S. L. McCall, and T. N. C. Venkatesan, "Differential gain and bistability using a sodium-filled Fabry–Perot interferometer," *Phys. Rev. Lett.* **36**, 1135–1138 (1976).
8. H. M. Gibbs, S. L. McCall, T. N. C. Venkatesan, A. C. Gosard, A. Passner, and W. Wiegmann "Optical bistability in semiconductors," *Appl. Phys. Lett.* **35**, 451–453 (1979).
9. D. Pellat, R. Azoulay, G. Leroux, L. Dugrand, Y. Rafflé, R. Kuzelwicz, and J. L. Oudar, "Optical bistability at 980 nm in a strained InGaAs/GaAs multiple quantum well microcavity with resonant periodic nonlinearity," *Appl. Phys. Lett.* **62**, 2489–2491 (1993).
10. A. Szöke, V. Daneu, J. Goldhar, and N. A. Kurnit, "Bistable optical element and its applications," *Appl. Phys. Lett.* **15**, 376–379 (1969).